Journal of Geophysical Research: Solid Earth

Supporting Information for

Nature of the Mantle Plume under the Emeishan Large Igneous Province: Constraints from Olivine-hosted Melt Inclusions of the Lijiang Picrites

Lei Zhang[1,2,3], Zhong-Yuan Ren[1,2,4*], Le Zhang[1,2], Ya-Dong Wu[1,4,5], Sheng-Ping Qian[1,6], Xiao-Ping Xia[1,2,4], and Yi-Gang Xu[1,2,4]

[1] State Key Laboratory of Isotope Geochemistry, Guangzhou Institute of Geochemistry, Chinese Academy of Sciences, Guangzhou, China

[2] CAS Center for Excellence in Deep Earth Science, Guangzhou, China

[3] College of Earth and Planetary Sciences, University of Chinese Academy of Sciences, Beijing, China

[4] Institutions of Earth Science, Chinese Academy of Sciences, Beijing, China

[5] State Key Laboratory of Lithospheric Evolution, Institute of Geology and Geophysics, Chinese Academy of Sciences, Beijing, China

[6] State Key Laboratory of Marine Geology, Tongji University, Shanghai, China

Corresponding author's E-mail address: zyren@gig.ac.cn

Contents of this file

Analytical methods, Supplementary Figures S1–S6

Additional Supporting Information (Files uploaded separately)

Table S1–S13. Data reported in this study and analytical errors.

Table S14. The parameters used in isotopic modeling.

Table S15. The parameters used in the Tp calculation

Introduction

The supporting information includes analytical methods, 6 figures and 15 tables. All data in Tables S1-S13 were obtained in this study with the analytical and calculation methods described in the text. Table S14 is the modeling parameters used in Figure 10. Table S15 is the parameter used in the Tp calculation.

S1. Whole-rock major and trace elements for the Lijiang picrites, Emeishan LIP
S2. Whole-rock Sr–Nd–Pb–Hf isotope ratios for the Lijiang picrites, Emeishan LIP
S3. Raw major element compositions of melt inclusions in the Lijiang picrites
S4. Calculated compositions of melt inclusions and forsterite contents of their host olivines from the Lijiang picrites, Emeishan LIP
S5. Compositions of olivine phenocrysts from the Lijiang picrites, Emeishan LIP
S6. Raw trace element compositions of melt inclusions in the Lijiang picrites
S7. Trace element and Pb isotope compositions of the Lijiang melt inclusions
S8. Major element compositions of primary magma for the Lijiang and Dali picrites
S9. Trace element compositions of primary magma for the Lijiang picrites
S10. Compositions of Cr-spinel inclusions and their host olivines in the Lijiang and Dali picrites, Emeishan LIP
S11. Standard results for whole rock isotope analysis
S12. Standard results for trace element analysis by SIMS
S13. Standard results for Pb isotope analysis by LA-MC-ICP-MS
S14. The modeling parameters used in isotopic modeling of Figure 10
S15. The parameters used in the Tp calculation

Analytical Methods

First, the weathered surface of Lijiang picrites were removed, and then cut the samples into 0.3–0.5 cm chips. The freshest chips of approximately 80 g were carefully selected, and then washed in Milli-Q water three times before milling. These samples were dried and ground into 200 mesh powders with a disc pulverizer. The pulverizer was thoroughly cleaned with water and quartz sand between each sample.

All analyses were conducted at the State Key Laboratory of Isotope Geochemistry, Guangzhou Institute of Geochemistry, Chinese Academy of Sciences (GIG-CAS).

Whole-rock major and trace elements

Whole-rock major element compositions were analyzed using a Rigaku RIX-2000 X-ray fluorescence spectrometer (XRF) system. The analytical precision was generally better than 4% (2RSD) for major elements. Whole-rock trace element compositions were determined on a Thermo Fisher iCAP inductively coupled plasma mass spectrometer (ICP-MS). Approximately 40 mg of whole-rock powder was digested using a HNO_3+HF+$HClO_4$ mixture in a Teflon bomb for 48 hours at 100°C and then evaporated to dryness. Next, the residue was digested with HNO_3+HF+$HClO_4$ mixture in a high-pressure Teflon bomb that was sealed in a stainless steel bomb at 190°C for 48 hours. Rh was used as an internal standard to monitor instrumental drift during measurement. The USGS standards BHVO-2, AGV-2, W-2, and Chinese national igneous rock standard materials GSR-1, GSR-2, and GSR-3 (Xie et al., 1989) were used for external calibration to calculate the element concentrations. The analytical precision of rare earth elements (REEs) and other incompatible elements was generally better than 6% (2RSD). (The data are supplied in Supplementary Table S1.)

Whole-rock Sr–Nd–Pb–Hf isotopes

The picrites and basalts in the Emeishan LIP are generally altered (Li et al., 2010; Ren et al., 2017; Zhang et al., 2006), as they are in Lijiang (Fig. S1). Thus, an acid leaching process was used during sample preparation to remove secondary phases or potential contamination. The leaching followed the procedure in Weis et al. (2005). Approximately 0.4 g of sample powder was placed in a 15 mL Teflon beaker. The weighted sample was ultrasonicated in 6N HCl for 20 minutes, and the supernatant was then decanted. The above procedure was repeated 5 times until the supernatant was clear. The processed samples were ultrasonicated in Milli-Q water 2 times before isotope analysis. We also analyzed the trace element compositions of the picrites after

leaching to determine the P/D ratios for isotope calculation.

Whole-rock Sr–Nd–Pb–Hf isotope compositions were analyzed on a Neptune Plus MC-ICP-MS. Nd and Sr isotope ratios were normalized to $^{146}Nd/^{144}Nd = 0.7219$ (Vance & Thirlwall, 2002) and $^{86}Sr/^{88}Sr = 0.1194$ (Elburg et al., 2005), respectively, for mass fractionation correction. During the analysis, the average values of repeated measurements of standard NIST SRM 987 for $^{87}Sr/^{86}Sr$ were 0.710257 ± 0.000013 (2SD, n=5), standard JNdi-1 for $^{143}Nd/^{144}Nd$ were 0.512109 ± 0.000014 (2SD, n=5), standard JCM14374 for Hf isotope were 0.282189 ± 0.000010 (2SD, n=5), which were consistent with the recommended values of 0.710244 (Elburg et al., 2005), 0.512115 (Tanaka et al., 2000), and 0.282189 (Wu et al., 2006), respectively. The reproducibility of Pb isotope analysis was monitored by repeated analyses of NIST SRM 981 and produced $^{206}Pb/^{204}Pb$, $^{207}Pb/^{204}Pb$, and $^{208}Pb/^{204}Pb$ ratios of 16.9336 ± 0.0022, 15.4875 ± 0.0016 and 36.6892 ± 0.0055 (2SD, n=5), which were consistent with the recommended values of 16.935, 15.4890, and 36.7070, respectively (Todt et al., 1996). The measured Pb isotope composition was corrected for U–Th decay and age-corrected to 260 Ma. (The data are supplied in Supplementary Table S2, and analytical results for the standards are supplied in Supplementary Table S11.)

EPMA analysis of olivines, melt inclusions, and spinel inclusions

The sample chips were crushed by a SELFRAG pulsed power selective fragmentation instrument to separate olivine grains. Olivine grains were handpicked from crushed chips using a binocular microscope and to make sure the olivines are fresh and without alteration. All selected melt inclusions were in regular shape, do not show dark appearance, and had no fractures or breaches. Melt inclusions smaller than 25μm were not used because of the potential boundary layer effect. Because natural cooling of melt inclusions after trapping would result in crystallization of olivine and other daughter minerals, a homogenization process is required. Olivine grains of each sample were homogenized using a vertical gas-mixing furnace at 1 atm with a temperature of 1250°C, and the quartz-fayalite-magnetite oxygen buffer condition was maintained by a CO_2–H_2 gas-mixing system. Olivines were wrapped into a Pt capsule and gradually lowered to the heating position (1250°C) from the top of the furnace over 10 minutes and sustained at this temperature for another 10 minutes. The homogenized olivine grains were then mounted in epoxy and polished carefully until inclusions were exposed on the surfaces for subsequent *in situ* analysis (Ren et al., 2005, 2017). In addition, we mounted unheated olivine grains of each sample in epoxy

resin and polished them to expose spinel inclusions. All selected spinels were larger than 8 μm and had no fractures.

The major elements of the melt inclusions were determined on a JEOL JXA-8100 Superprobe with the following operating conditions: accelerating voltage of 15 kV, beam current of 20 nA, and spot diameter of 3 μm. Na and K were analyzed first to minimize their losses. To monitor instrumental drift, an international glass standard GSD-1G (Jochum et al., 2011) was analyzed, with precision (2RSD) better than 2.8% for SiO_2, Al_2O_3, FeO, CaO, better than 3.8% for MgO, better than 6.9% for TiO_2, Na_2O, K_2O, P_2O_5, and better than 37.8% for MnO. For each melt inclusion, we analyzed 1-3 points and calculated the average composition. (The major elements of the melt inclusions are supplied in Supplementary Table S3.) The major elements of the spinel inclusions were analyzed with a JEOL JXA-8100 Superprobe under the following operating conditions: accelerating voltage of 15 kV, beam current of 20 nA, and spot diameter of 1 μm. During measurements, each spot was analyzed separately, and the focus was manually adjusted to achieve a good state. The spinel standard BAR601-10 were analyzed during measurements. The external precisions (2RSD) for the elements were 2.1% (Al_2O_3), 2.4% (Cr_2O_3), 2.7% (FeO), 2.1% (MgO), and accuracy were better than 1% for Al_2O_3, Cr_2O_3 and 3% for FeO, MgO (the reference composition are from Cao et al., 2019). (The major elements of the spinel are supplied in Supplementary Table S10.)

The host olivines of spinel and melt inclusions were analyzed with a JEOL JXA-8230 Superprobe. SiO_2, FeO, and MgO were analyzed with an accelerating voltage of 15 kV, a beam current of 20 nA, and a spot size of 1 μm. The trace elements in olivine (NiO, MnO, CaO, and Al_2O_3) were analyzed following the method of Sobolev et al. (2007), with an accelerating voltage of 20 kV, a beam current of 300 nA, and a spot size of 1 μm. The MongOL (Batanova et al., 2019) was analyzed after every 5 measurements to monitor potential instrumental drift and to estimate accuracy and precision. The external precisions (2RSD) for the elements were 0.36% (SiO_2), 0.48% (MgO), 1.3% (FeO), 1.9% (NiO), 3.1% (CaO), 1.8% (MnO), and 9.1% (Al_2O_3). (The data of olivines are supplied in Supplementary Tables S5 and S10.)

Melt inclusion trace elements

The trace element concentrations of melt inclusions were measured using a Cameca IMS 1280HR secondary ion mass spectrometry (SIMS). O_2^- was selected as

the primary ion to bombard the sample surface with a current of 4–10 nA. The size of the ion spot on the sample surface was approximately 20 μm × 30 μm. The secondary accelerating voltage was 10 Kv, and the molecular interferences were filtered by an offset of 50±10 eV. The mass resolution was set to 8000 to separate most mass interferences. Peak positions were verified before each analysis, and a mass of 130.5 was scanned as background in each cycle and was always less than 0.1 cps. Each analysis consisted of 60 s pre-sputtering followed by 8 cycles of peak hopping scanning. All measured element intensities were normalized to ^{29}Si, and a multistandard linear correction was performed for each element using GSC-1G, BHVO-2G, TB-1G, BCR-2G, and BIR-1G to convert ion intensities to concentrations. To monitor instrument drift and the accuracy of the result, the basaltic glass standard GSD-1G was analyzed after every three spots. Twenty analyses of GSD-1G indicated that all measured elements had precisions better than 10% (2RSD), and that except for Eu (15.8%), the accuracies of all other measured elements were within ±8% of their recommended values. (The data are supplied in Supplementary Table S6, and analytical results for GSD-1G are supplied in Supplementary Table S12.)

***In situ* Pb isotope analysis of melt inclusions**

After trace element measurement, the sample mounts were carefully polished, ultrasonically cleaned with purified 1% HNO_3 and Milli-Q water and then dried with N_2 gas flow. The Pb isotope analysis of melt inclusions was performed with a Neptune Plus MC-ICP-MS coupled with a RESOlution M-50 193 nm laser ablation system. Eight ion counters were used to collect each isotope signal under static mode. A jet sample cone and an X skimmer cone were used at the interface to enhance signal intensity (Zhang et al., 2014). The laser parameters were set as follows: spot size, 40 μm; energy density, ~4 J/cm^2; repetition rate, 3 Hz. Each spot analysis consisted of 30 s gas blank collection with the laser off and 30 s sample signal collection with the laser on. Due to the low Pb contents (less than 3.5 ppm) of the measured inclusions and the significant isobaric interference of ^{204}Hg on ^{204}Pb, Pb isotope ratios related to ^{204}Pb were not considered in this study. Before each spot analysis, pre-ablation was conducted to avoid potential contamination on the sample surface. The USGS reference glass NKT-1G was used as the external calibrator. The precision and accuracy were evaluated by repeated analyses of the standard glass BHVO-2G. The precisions of $^{208}Pb/^{206}Pb$ and $^{207}Pb/^{206}Pb$ were 2.052±0.005 and 0.833±0.002 (2SD), respectively, comparable with the recommend value of 2.052 and 0.834 (Weis et al.,

2005). The accuracies of $^{208}Pb/^{206}Pb$ and $^{207}Pb/^{206}Pb$ were better than 0.03% and 0.16%, respectively. The measured Pb isotope compositions were corrected for U–Th decay and age-corrected to 260 Ma. (The data are supplied in Supplementary Table S5, and analytical results for BHVO-2G are supplied in Supplementary Table S13.)

Supplementary Figures S1–S6

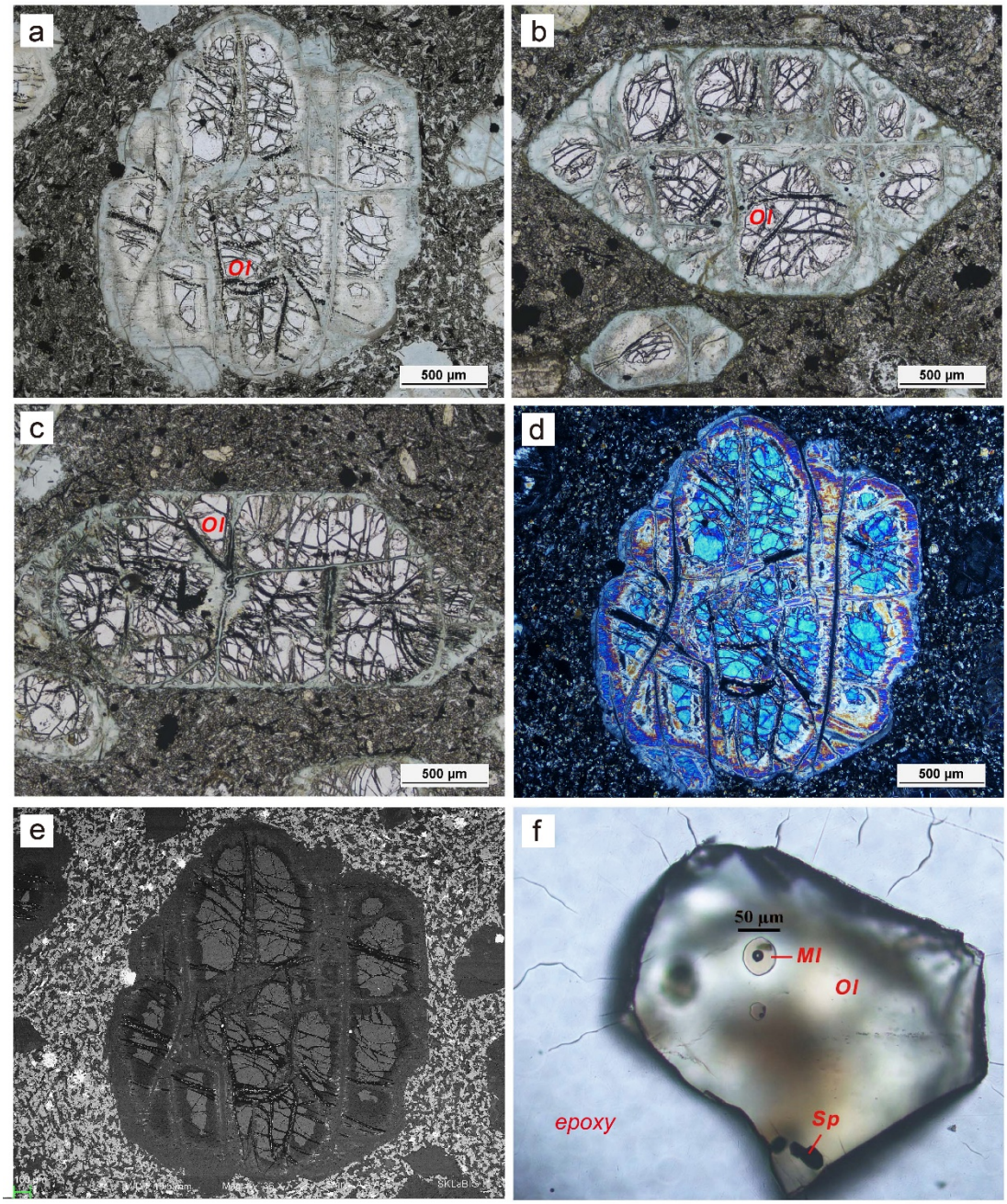

Figure S1. Photomicrographs of Lijiang picrites and olivines. (a-d) and (f) are in transmitted light, (d) are in cross-polarized ligh, (e) are backscattered electron image of olivine. (a, e) Serpentinization and chloritization occur along the rims and fractures of olivine (Ol), and unaffected olivine cores remain. (b, c) Euhedral olivine crystal forms remain. (f) Melt inclusions (MI) after homogenization. The olivines were mounted in epoxy and polished until inclusions were exposed at the surfaces. Fine-grained euhedral Cr-spinel (Sp) is enclosed in olivine.

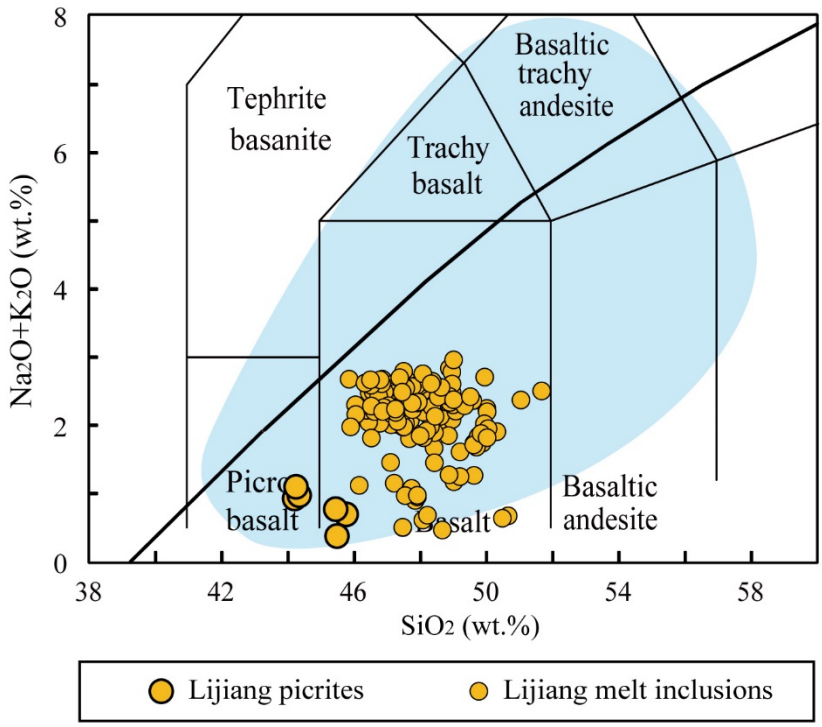

Figure S2. $Na_2O + K_2O$ versus SiO_2 (wt.%) classification diagram for Lijiang melt inclusions and host picrites. Compositional fields are from Le Bas et al. (1986). All Lijiang melt inclusions plot in the sub-alkaline series. The light-blue field is based on the compositions of all picrites and basaltic rocks from the Emeishan LIP.

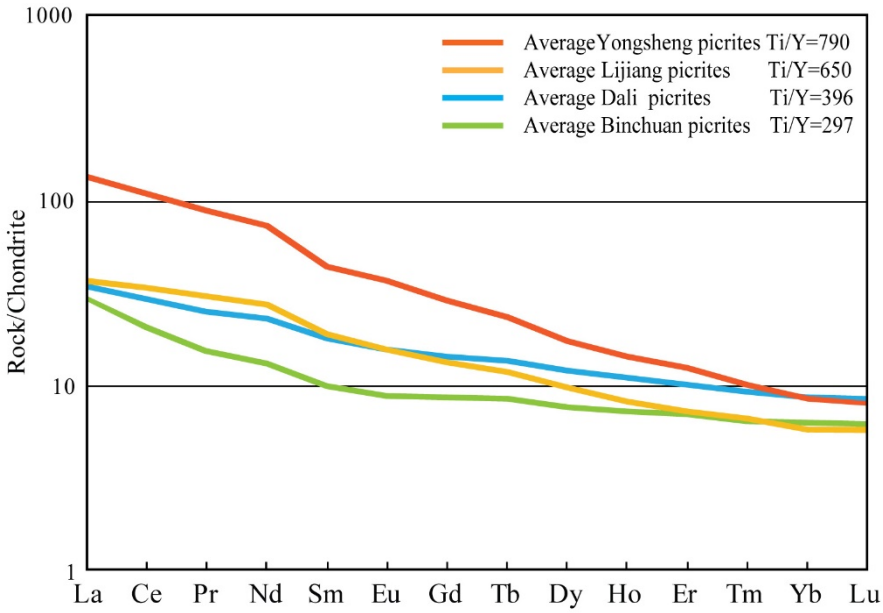

Figure S3. Chondrite-normalized rare earth element (REE) patterns for major picrites in the Emeishan LIP. Lijiang picrite compositions are from this study. The picrites compositions for Binchuan and Yongsheng are from Kamenetsky et al. (2012), and the picrite compositions for Dali are from Wu et al. (2018). The chondrite values are from Sun and McDonough (1989).

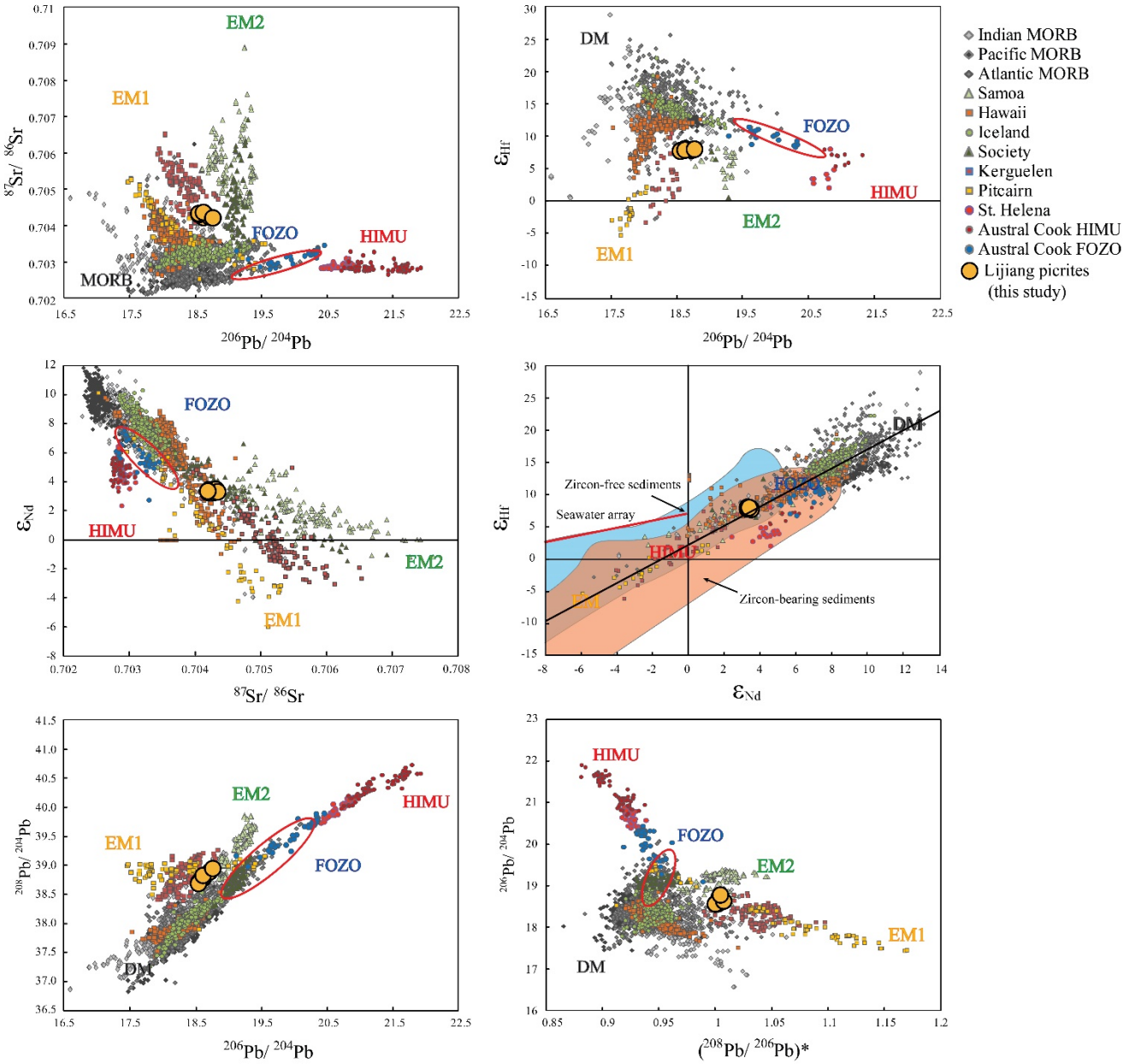

Figure S4. Sr–Nd–Pb–Hf isotope characteristics of Lijiang picrites (large yellow circles). The Lijiang isotope compositions shown in these figures are initial isotope compositions corrected to 260 Ma. The compositions of typical global OIBs and MORBs are also plotted for comparison. Data for global OIBs and MORBs are from Stracke (2012) and are not age-corrected to 260 Ma. The compositional fields of zircon-free sediment and zircon-bearing sediment in the ε_{Nd}–ε_{Hf} plot are from Bayon et al. (2009). Seawater array are from Vervoort et al. (2011). $(^{208}Pb/^{206}Pb)^*$ is defined by the equation $(^{208}Pb/^{206}Pb)^* = (^{208}Pb/^{204}Pb_{measured} - 29.476)/(^{206}Pb/^{204}Pb_{measured} - 9.307)$ (Galer & O'Nions, 1985). The mantle array in the $\varepsilon_{Nd(t)}$ –$\varepsilon_{Hf(t)}$ plot is from Jourdan et al. (2007).

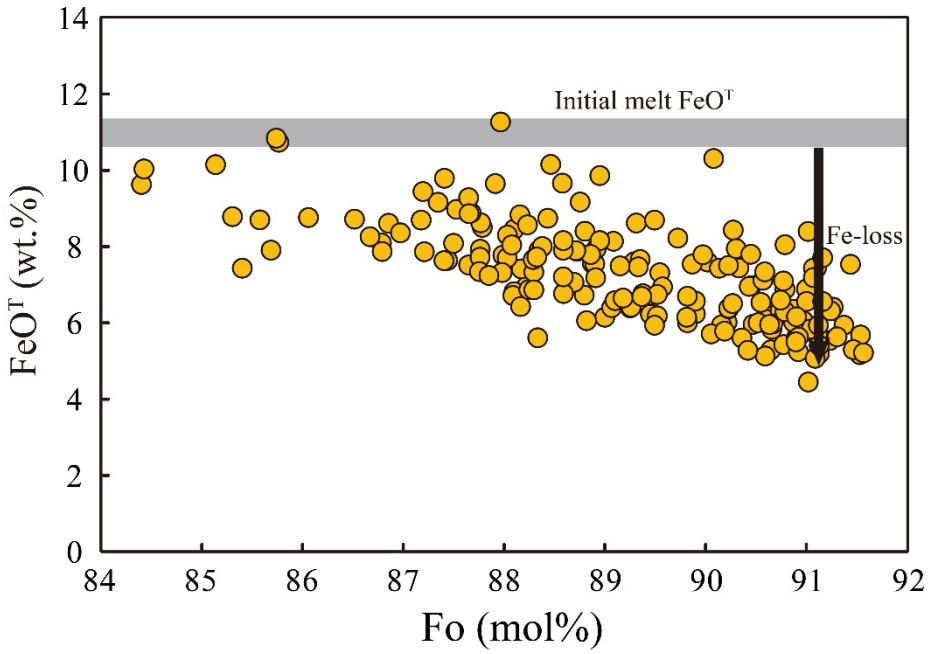

Figure S5. FeO^T for uncorrected olivine-hosted melt inclusions composition of Lijiang picrites against Fo values of host olivines.

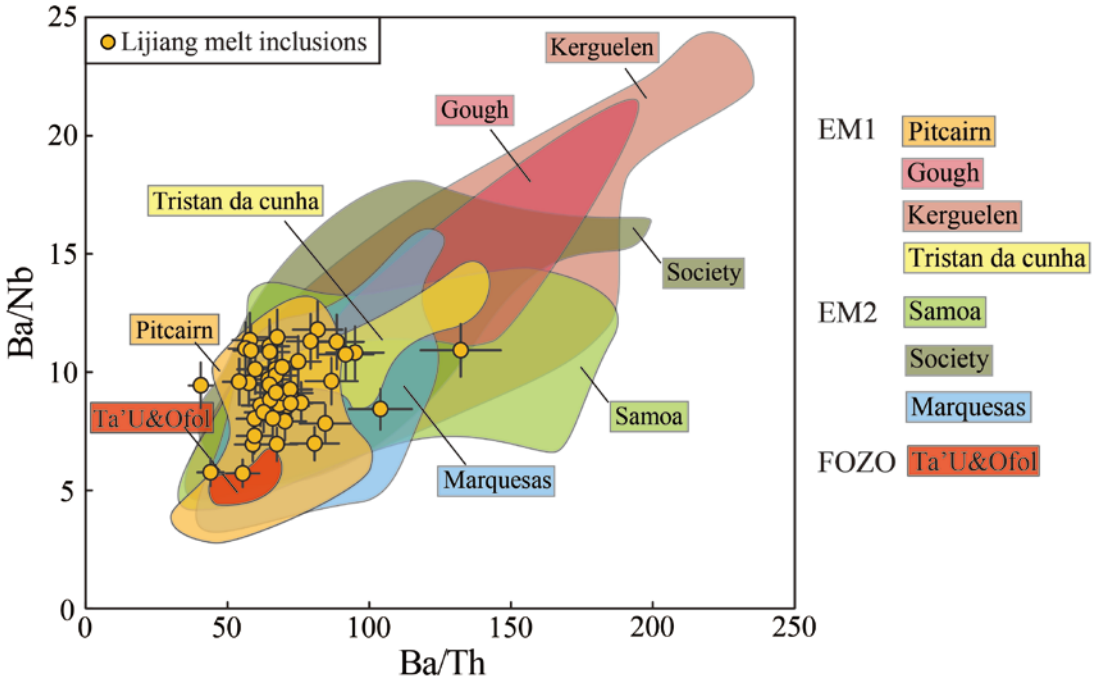

Figure S6. Comparison of Lijiang melt inclusion compositions with typical oceanic island basalts on Ba/Nb versus Ba/Th plot. Compositional fields of typical OIBs are compiled from GEOROC (http://georoc.mpch-mainz.gwdg.de/).